Lung Segmentation of Chest Radiograph Using Circular Window Based Local Contrast Thresholding (CWLCT) and Adaptive Median Outlier (CWAMO)

Dnyaneshwar Kanade*, *Jagdish* Helonde, *Prakash* Burade, *Mangesh* Nikose

Department of Electrical & Electronics Engineering, School of Engineering and Technology, Sandip University

Abstract. Certain chest illnesses, such as TB, adenocarcinoma, squamous cell carcinoma, large cell carcinoma, atelectasis, etc., can be diagnosed in chest radiographs, and the development of a CAD system relies in part on accurate lung segmentation. In order to partition the lungs in chest radiographs, this work introduces an unsupervised learning approach based on a circular window and local thresholding. The procedure involves pre-processing, a preliminary estimate of the lung field, and the elimination of noise. Images are initially scaled down to 1024x1024 and enhanced using adaptive histogram equalization. Then chest radiographs are binarized using the proposed method. Based on the geometrical and special characteristics, lungs are separated from the chest radiographs. The final step in picture segmentation is the use of morphological processes. Local thresholding, omitting extraneous body parts, filling in gaps, and filtering regions based on their attributes all contribute to preliminary estimates of the lung field.

Morphological processes are used as a means of eliminating background noise. A public bone shadow eliminated JSRT dataset consisting of 247 chest x-rays is used to measure the performance of the proposed method. The effectiveness of the proposed method results' performance is evaluated by comparing it with Active Shape Model (ASM) based lung segmentation for various performance metrics such as F-score, overlap percentage, accuracy rate, sensitivity, specificity, and precision rates. All the parameters for the proposed method are over and above 90%. Our investigations indicate that the suggested method is an unsupervised learning approach that does not require any training.

Keywords: Keywords— Lung cancer, chest radiograph, Local Contrast thresholding

1. Introduction

Radiography, magnetic resonance imaging (MRI), and computed tomography (CT) are only few of the imaging modalities frequently used in medical diagnostics with the goal of finding lung cancer. Despite the fact that MRI and CT are more sensitive and accurate techniques, chest radiography continues to receive the highest level of recommendation for

*dnyaneshwar.kanade@vit.edu

the initial diagnosis and screening of lung cancer due to its noninvasive nature, low radiation dosage, and reasonable cost. Chest radiology is still the most widely accepted way to find illnesses like lung cancer and tuberculosis in the chest. It's due to its being the most cost-effective, easiest for using, and best diagnostic tool. This is why it is one of the greatest problems in medical diagnostics to figure out how to spot such illnesses in their early or fragile stages on chest x-rays. Automation of x-ray illness detection has been the subject of extensive investigation in recent years. This helps find diseases earlier and gives patients a favorable survival.

In order to narrow the focus of the detection procedures, the x-rays of the lungs must first be separated into different areas. The system's overall performance is contingent on the results of how well this step is done, since incorrect lung categorization might lead to more misleading results. The proposed method uses Japanese Society of Radiological Technology (JSRT) database[1]. A fully automated method [2] is shown for processing digital postero-anterior (PA) chest x-rays, starting with accurate segmentation of the lung field area. Lung segments include those typically ignored by researchers since they are located behind the heart, spine, and diaphragm. Image thresholding techniques [3] were looked at in depth to classify them, define their formulas in a standard way, and compare how well they work. The shape of the histogram, the number of clusters in the measurement space, the entropy of the data, the properties of the object, the spatial correlation, and the local gray-level surface are all examples of information that may be used to classify the various thresholding strategies. In the context of non-destructive testing applications and document images, 40 thresholding methods from different categories are compared. Total performance indicators are used to compare the two things. Adaptive contrast equalization [4] and non-linear filtering are used to come up with a unique way to improve original photos. Then, morphological processes are used to get a rough estimate of lung area, which is then improved by expanding this area to get the exact final contour. We give a strong solution [5] for separating the lungs in traditional and mobile chest x-rays by using a completely unsupervised algorithm. This innovative technique refines the lung area using an oriented Gaussian derivatives filter with seven orientations, Fuzzy C-Means (FCM) clustering, and thresholding. The Residual block, the Efficientnet-b4 encoder, and the Leaky ReLU activation mechanism in the decoder are all proposed as ways to improve the U-Net network [6]. By avoiding the multiplication effect in gradient backpropagation, the network is able to obtain accurate data on the Lung field without experiencing any instability. On the basis of shadow filter and local thresholding [7], an unsupervised learning method for separating the lungs from chest x-rays was created. Metrics for how well the proposed method works are higher than 90%. Without supervision, a method based on a multiresolution fractal feature vector [8] is given. The lung field region is well described by the feature vector. Then, a good starting contour is produced using a fuzzy c-means clustering technique. Deformable models decide what the final shape will be. This algorithm works very well, but this study only has a small number of samples to look at. Using a hybrid method that combines distance-regularized level set and deep structured inference, a new strategy [9] is proposed for separating the lungs in CXR images. This plan was made so that it could be used. This combination combines the benefits of deep learning methods and level set methods. Deep learning methods have a few advantages. Two of them are robust training with few annotated samples and top-down segmentation with structured inference and learning (use of shape and appearance priors and efficient optimization techniques). When their methods are used on the JSRT dataset, they get an average accuracy of between 94.8 and 98.8%. An accurate method for pinpointing lung borders, based on each individual's own lung atlas is proposed. This technique employs SIFT-flow nonrigid registration with refinement using a graph cuts segmentation strategy, and it makes advantage of quick partial Radon profile similarity selection [10]. In order to spot emphysema in chest x-rays, this article details a CAD method. The lung border is represented as a closed fuzzy-

curve [11] to segment the lung field in both posteroanterior (PA) and lateral computed tomography (CXR) images. After the intensity profile is processed, an optimization is done on a flexible polynomial template that was made without any training data [12]. Due to the shadow of the heart and changes in the shape of the lungs, the right and left lungs are processed separately. Processing intensity profiles involves finding the highest and lowest points in horizontal profile segments or their derivatives. In binarization, the threshold is an important factor. So, choosing the right threshold value in binarization is an important part of making a good binary image. There are two ways to do this: global thresholding and local thresholding. [13] talks about a local thresholding strategy that uses the local contrast and mean. Normal front-to-back chest x-rays require the reader to make mental distinctions between the lung fields, heart, and clavicles. Active structure models, active appearance models, and a multi-resolution pixel categorization approach based on a multi-scale filter bank of Gaussian derivatives and a k-nearest-neighbors classifier are all compared as guided methods for segmentation [14]. The approaches were judged using a database of 247 chest x-rays that was available to the public and in which all the objects were separated by hand by two human observers. Using the local mean [15] and standard deviation, a method is made that gets rid of background noise called locally adaptive thresholding. A detailed look at the pros and cons of the different segmentation techniques [16] was given. Different techniques for region-based segmentation and segmentation based on edge detection [17] were looked at and compared. In the section on region-based techniques, we talked about thresholding, region growing, and the watershed algorithm. Edge detection and segmentation techniques talked about the canny edge detector and the active contour algorithms. A fully automatic method [18] for recognizing lungs in CT scans is presented. There are three primary components to the strategy. To begin, CT scans had their lung regions removed using gray-level thresholding. The front and back connections are then used to dissect the lungs apart into their left and right halves [19]. The lung edge is then sharpened along the middle of the chest. Suggested lung segmentation begins with lung edge identification using canny edge detection filters, Euler number methodology, and morphology method. In this experiment, it was hard to find a good low and high threshold value for detecting sharp edges. Because of this, the Euler number was used to make the detection process easier. Their unsupervised segmentation algorithm still can't find the lung region correctly. In an iterative framework, a technique is proposed [20] for segmenting lung fields by merging prior shape information with intensity-based thresholding. This method for doing experiments worked well. But the method has two problems: I it needs human experts to figure out the shape of the lung model, and (ii) it can't find the lung tissues that overlap with the heart because the intensity changes in this area. For the automatic segmentation of the lung field in chest x-rays, a fuzzy clustering method based on a Gaussian kernel [21] and spatial constraints is suggested. An Active Shape Model (ASM) is a computer vision technique used to identify and track objects in images [22] – [25]. It is based on a statistical model of the shape of the object, which is used to search for the object in an image. The model is made from a set of training images that are used to make a statistical model of the shape of the object. Then, the model is used to find the object in an image by comparing the shape of the object in the image to the shape of the object in the model. [26] Someone came up with a way to make small models of the shape and look of flexible things (like organs) that can be seen in two-dimensional photographs. The models are made by looking at the numbers of images that have been labeled with examples of the things that were labeled. Each model is made up of a flexible form template and a statistical model that says how grey the area around each model point should look. A new way to separate the lungs from digital Posterior-Anterior (PA) chest x-ray images is shown in [27]. This method uses a level set. When using active contours to divide the lungs, the biggest problem is local minima caused by shading effects and the fact that the rib cage and clavicle make the edges very sharp. The method used the fact that there

was good contrast at the edges of the lungs to get a set of edge/corner feature points with different sizes. Our active contour model was then based on these features. By using the lung ROI to get the translation and scaling parameters, a method [28] was made to predict an appropriate initial lung border for ASM deformation. Using k-means clustering and silhouette-based cluster validation, an adaptive ASM was made to change as the shape of the lung changed. This was done to get around the fact that everyone's lung shape is different. Experiments showed that adaptive ASM segmentation works better than traditional ASM segmentation techniques. A unique method [29] is shown to make the original ASM more resistant to weak lung field edges, which can cause the contour to leak into the lung fields. The ASM is protected from leakage by a grey-level selective thresholding system that subtracts unnecessary anatomic features from the radiograph. The suggested method works with affine lung field projections and doesn't get messed up by things that are used to monitor and support the patient that are dense [30]. Contrary to the original formulation, an active shape model segmentation approach is described that is guided by optimal local features rather than normalized first-order derivative profiles. Instead of using the linear Mahalanobis distance, a nonlinear kNN-classifier is used to figure out how far apart landmarks should be. At each resolution level considered during the segmentation optimization technique, a distinct set of optimal features is determined for each of the shape-describing landmarks. Automatic feature selection is done with the help of training images and forward and backward feature selection in a certain order. A new way to do things that involves two main steps [31]. First, the shape of the lungs is roughly divided into different parts using a new method called robust active shape model (RASM) matching. A rib cage detection method is used to find where the RASM is at first. Second, a method for finding the best surface is used to make the first result of segmentation fit the lung even better. Both the left and right lungs have their separate parts.

2. Materials and methods

2.1. Assumptions

The following are presumptions that must be made before the suggested approach for lung segmentation from chest radiographs may be used:

1) Digital x-ray images are taken from the JSRT bone shadow eliminated dataset developed at Budapest University (BSE_BU). There are a total of 154 chest x-rays with lung nodules and 93 without lesions in the sample.

2) For comparing the proposed method results, the Active Shape Model (ASM) lung masks and manually segmented lungs mask using image-J software are used.

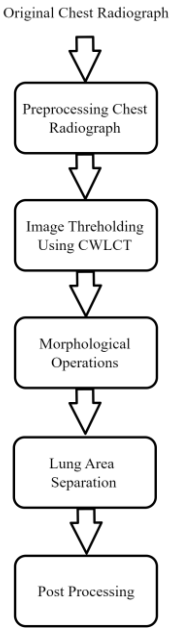

Fig. 1. System Flow Chart

2.2. Algorithm

As shown in Figure 1, the proposed system consists of five different stages namely-1) Preprocessing 2) Image thresholding using CWLCT 3) Morphological Operations 4) Lung area separation 5) Post processing.

2.2.1. Preprocessing of the chest radiograph

Prior lung segmentation the images are preprocessed for better results. The images are down sampled to 1024x1024 and enhanced for their contrast using adaptive histogram equalization.

2.2.2. Image thresholding using CWLCT

The preprocessed images are then binarized [32] using circular window based local contrast thresholding. For the binarization CWLCT filter with radius 50 and threshold 2 is employed. The CWLCT filter is similar to Bernsen local contrast thresholding filter. Instead of using square window, it uses circular filter detecting the curved boundary regions of the lungs. Calculating the median of the pixel intensities in the image region that was covered by the circular window required centering the circular window at the pixel with the coordinates f(x,y). If the pixel intensity at f(x,y) is higher than that of the median value by the threshold value t, then the standard deviation will be used as the threshold value, and the median value will be used to substitute the pixel intensity at f(x,y); else, the pixel intensity will be left at its original value.

$$I_1(x,y) = \begin{cases} m \;\; if \; I(x,y) > m + t \\ I(x,y) \qquad otherwise \end{cases} \tag{1}$$

Where *I(x,y)* is the intensity of the gray level when it was first

recorded at pixel *f(x,y)*, and *I1(x,y)* is the intensity of the gray level after it has been updated at pixel *f(x,y)*. Figure 2a shows

original image while Figure 2b shows thresholded image using CWLCT.

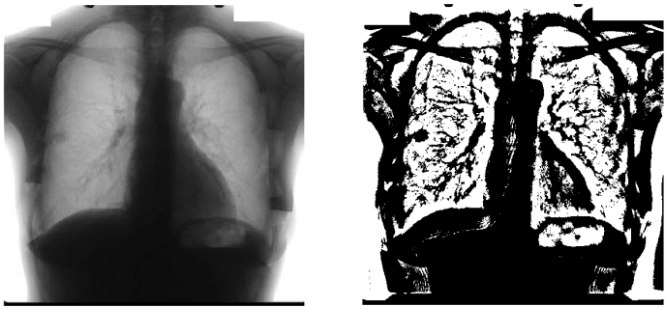

a b

Fig. 2. Image thresholding using CWLCT a) Original image b) Thresholded image

2.2.3. Morphological operations

In the morphological operation a combination of dilation followed by erosion is used to fill in small holes or gaps in an

image, or to smooth the edges of larger objects. Figure 3c shows the image after morphological operation.

a b c

Fig. 3. Morphological operation a) Original image b) Thresholded image c) Image after morphological operation

2.2.4. Lung area separation from chest radiograph

By using geometrical and spatial properties of the segmented parts of the chest radiograph, left and the right lungs are separated. First all the segmented parts of the chest radiograph are labeled as shown in Figure 4b and then the centroid and the areas are calculated. The first two of the segmented parts having largest area and smallest Euclidean distance as shown in Figure 4c from the center of the image are separated. Since the left and right lungs are the parts having larger areas as compared to the other labeled parts and closer to the center of the image, they are separated easily.

a b c

Fig. 4. Lungs Separation a) Thresholded image b) Labeled image c) Image after lung separation

2.2.5 Post Processing

In the post processing the Bottom Hat filter and adaptive median outlier filter[32] is used. The Bottom Hat filter is a morphological operation that is used in image processing to enhance dark and low-contrast features in an image. It is a type of filtering that extracts the information contained in the darker regions of the image. The Bottom Hat filter is obtained by subtracting the original image from its morphological closing operation. The closing operation is performed by dilating the image and then eroding it with a structuring element. This operation removes small details and smooths the image. The result is then subtracted from the original image, which emphasizes the darker regions and small details that were removed in the closing operation.

$$Bottom_{hat}\,(f) = (f \cdot Y) - f \tag{2}$$

$$= Close(Image) - Image \tag{3}$$

Where, f is the original image and $\cdot$ the closing operator.

The bottom-hat filter has the property of enhancing "valleys" by applying the closing operator. The resulted image in Figure 5b is obtained by subtracting the image in Figure 4c from the original image in Figure 5a. Figure 5c is obtained after thresholding the image shown in Figure 5b.

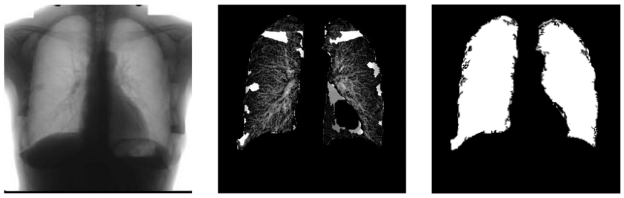

a b c

Fig. 5. Post Processing using Bottom hat filter a) Original image b) Bottom hat filtered image c) Binarized Image

After Bottom Hat filter segmented lung are further smoothed by using circular window based adaptive median outlier filter (CWAMO). The Figure 6b shows the final segmented lungs.

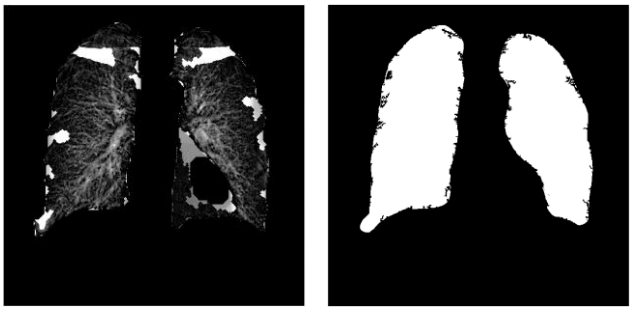

a b

Fig. 6. Post processing using CWAMO a) Original image b) Filtered image using CWAMO

3. Results and discussion

The performance analysis of the proposed method is done by comparing it with the lung segmentation using Active Shape Model (ASM). Active Shape Model (ASM) [22]is used for segmenting the lungs from the pre-processed original chest radiograph. When it comes to segmenting images, ASM is one of the most reliable algorithms available. Parameterized contour analysis is the focus of the Active Shape Model. The parameters are calculated using principal component analysis (PCA) and the statistics of many sets of points extracted from various contours of similar pictures. In ASM, an object's border is established by a set of n points. The resulting descriptor vector may be written as

$$x = (x_1, y_1, x_2, y_2, \ldots, x_n, y_n)^T \tag{4}$$

Where x_i and y_i are x and *y* coordinates on *i-th* point on the contour. The s training vectors calculated for principal component analysis have a mean shape of

$$\bar{x} = \frac{1}{s}\sum_{i=1}^{s} x_i \tag{5}$$

The covariance matrix will be

$$S = \frac{1}{1-s}\sum_{i=1}^{s}(x_i - \bar{x})\,(x_i - \bar{x})^T \tag{6}$$

The first *t* largest Eigen values λ_i of the covariance matrix are chosen. Because only the most significant Eigen values are considered, the number of parameters is drastically reduced and falls below n. The matrix is filled with the corresponding eigenvectors. The model parameters are calculated as

$$b = \Phi^T(x - \bar{x}) \tag{7}$$

from this the approximation of the shape is calculated as

$$x \approx \bar{x} + \Phi b \tag{8}$$

An appropriate b vector is identified for a given contour such that all components of b are within the interval $\pm m\sqrt{\lambda i}$, with an appropriate constant *m*. The parametric description of an object's contour is searched starting with the mean shape. Two alternating steps are applied until convergence or a predetermined number of iterations are reached. In the first phase of the method, each contour point perpendicular to the contour is moved. The optimal position is found after multiple cycles of position testing on both sides of the contour. During the training model, picture resolution is employed to locate the optimal position of an intensity gradient profile at each contour node. Finally, Mahalanobis distance is used to identify the optimal new position for the contour point. Then, to fit a model to the new point set, all of the contour points are updated. According to Eq.8, the best b parameter is sought

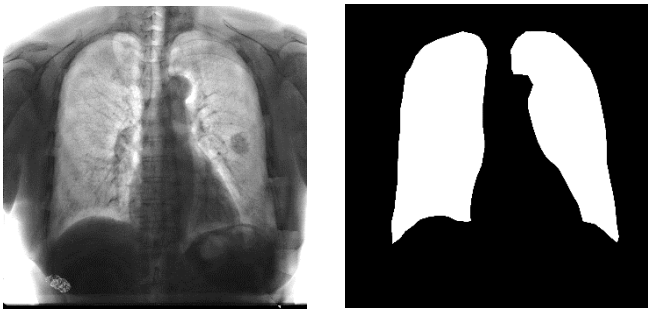

a b

Fig. 7. Lung segmentation using ASM a) Original image b) Segmented lungs using ASM

As the image's spatial resolution increases, the procedure is repeated many times. For training the model 100 images from the JSRT dataset are used [1].
Figure 7a shows original chest radiograph. The segmented lung mask obtained using ASM is shown in Figure 7b.
Figure-8 shows lung segmentation comparisons for sample images using proposed method and ASM. The segmented lung masks using proposed method are overlayed on the original images with green color while the lung segmented mask using ASM are overlayed on original images with red color. From the Figure-8 it can be observed that the lung segmentation using proposed method performs over and above the ASM which is one of the most rigid lung segmentation techniques.

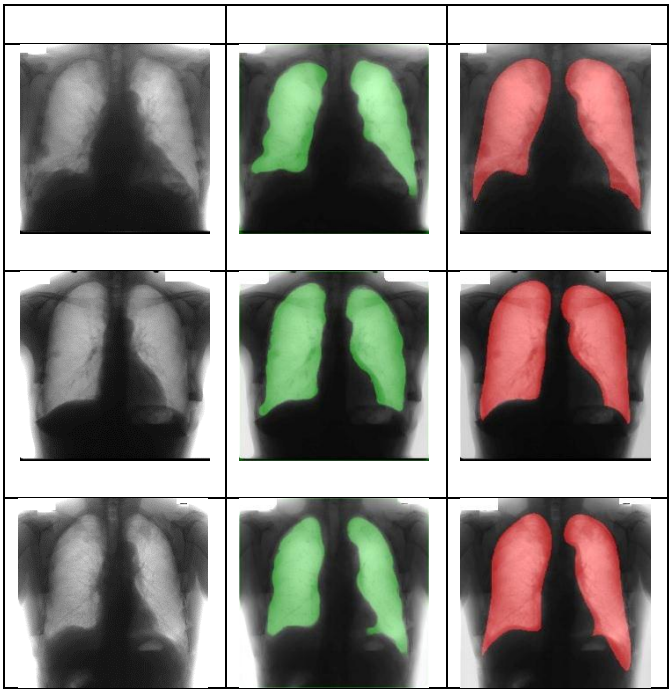

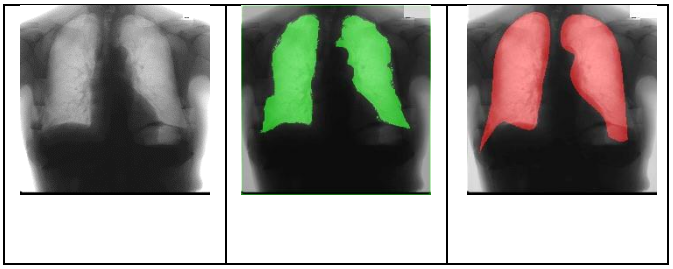

a b c

Fig. 8. Lung segmentation of sample images by using proposed method and ASM a) Original Images b) Lung segmentation using proposed method c) Lung segmentation using ASM)

To prove the results obtained in the Figure-8, 50 images from the JSRT dataset were used. The lungs are segmented using ASM (Supervised method) and proposed method (Unsupervised method). The lung masks are generated manually using ImageJ tool. These manually generated lung masks are verified using clinical experts and further used for evaluating the performance of the proposed method in comparison with the existing ASM algorithm.

The performance of the proposed method is evaluated using following measures

$$Accuracy = \frac{TP+TN}{TP+TN+FP+FN} \tag{9}$$

$$Specificity = \frac{TN}{TN+FP} \tag{10}$$

$$Sensitivity, R = \frac{TP}{TP+FN} \tag{11}$$

$$Precision, P = \frac{TP}{TP+FP} \tag{12}$$

$$Overlap,\ \Omega = \frac{TP}{TP+FP+FN} \tag{13}$$

$$F - Score = \frac{2 \times P \times R}{TP+FP} \tag{14}$$

Where TP is True Positive, TN is True Negative, FP is False Positive and FN is False Negative.

A "goodness" index is necessary for measuring the efficacy of the suggested strategy. True positive (TP) means the pixel belonging to foreground or lung is classified as lung pixel.

False positive (FP) means the pixel belonging to background is identified as lung pixel. False negative (FN) means pixel belonging lung classified as background and finally true negative (TN) means background pixel is correctly classified as background. The following formulae may be used to calculate values for overlap, accuracy, sensitivity, specificity, precision, and the F-score, all of which will be put to use in evaluating the quality of the results.

Table 1. Segmentation measure parameters comparison

Parameter	Lung Segmentation Using Proposed Method			Lung Segmentation Using ASM		
	Min	Max	Mean	Min	Max	Mean
Accuracy	0.9012	0.9721	0.9695	0.9213	0.9655	0.9434
Sensitivity	0.7235	0.9651	0.9371	0.7117	0.9632	0.9359
Specificity	0.7865	0.9915	0.9776	0.7971	0.9878	0.9712
Overlap	0.5934	0.9412	0.9110	0.6122	0.9231	0.9076
F-Score	0.7992	0.9642	0.9391	0.7567	0.9689	0.9213
Precision	0.7047	0.9812	0.9539	0.6710	0.9916	0.9518

Table I shows the comparison of segmentation using proposed method and ASM for different quality measures. From the table it can observed that using proposed method for lung segmentation the accuracy, specificity, and precision are above 95% and sensitivity, overlap and F-score lies above 90%. If we compare the results of the proposed method with the ASM lung segmentation technique, the proposed method gives over and above results. From the Figure 9 it can be observed that minimum percentage of image pixels correctly classified using ASM is greater than the proposed method. On the other hand, the mean and maximum percentage of image pixels accurately classified as lung area pixels using proposed method are greater than the ASM. Figure 10, Figure11, Figure 12, Figure 13 and Figure 14 show that the other image quality measures for the proposed method perform equal and above as that of the ASM lung segmentation method.

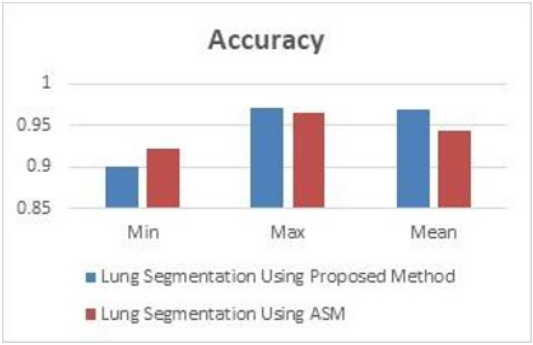

Fig. 9. Lung segmentation accuracy comparison

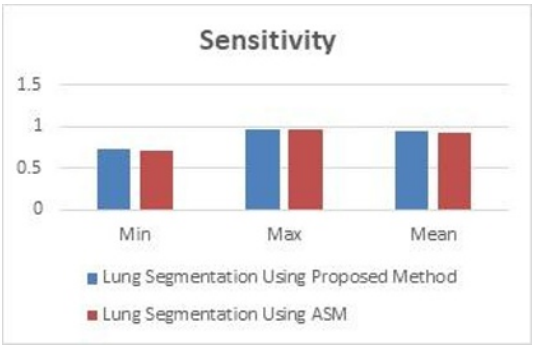

Fig. 10. Lung segmentation sensitivity comparison

Fig. 11. Lung segmentation specificity comparison

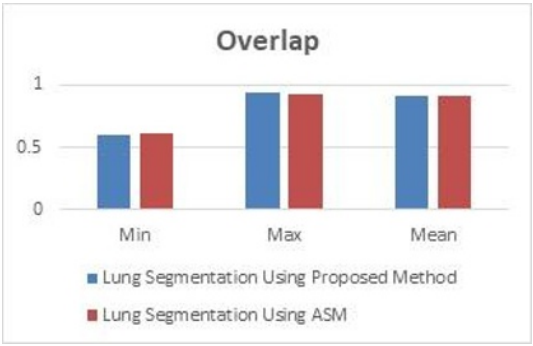

Fig. 12. Lung segmentation overlap comparison

Fig. 13. Lung segmentation precision comparison

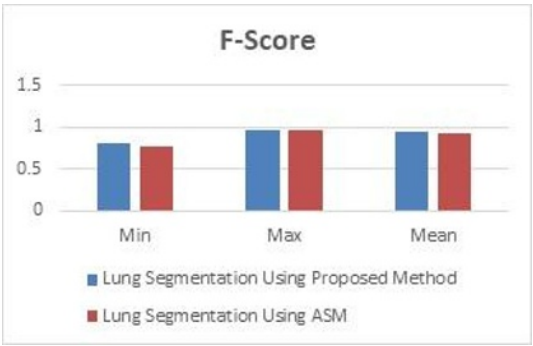

Fig. 14. Lung segmentation F-Score comparison

4. Conclusions and Future Work

Improved lung segmentation quality measures were the motivation for the proposed study of lung segmentation of chest radiographs utilizing the suggested approach (CWLCT & CWAMO). Using circular window based local contrast thresholding the lungs are segmented. Morphological operations such as to-hat window was employed for recovering the missing area. Finally, noise is reduced by applying the circular window based adaptive median outlier method. From the experimentation it can be concluded that by using proposed method for lung segmentation the accuracy, specificity, and precision are above 95% and sensitivity, overlap and F-score lies above 90%. For computing above parameters, manually segmented lungs that are verified by two medical experts are used. Since method is unsupervised, it does not require large image dataset and extensive effort for training the model. The results are compared with that supervised lung segmentation method (ASM) and it is found that for most of the parameters proposed method performs over and above the ASM.

5. References

1. S. Junji *et al.*, "A Development of a Digital Image Database for Chest Radiographs With and Without a Lung Nodule: Receiver Operating Characteristic Analysis of Radiologists' Detection of Pulmonary Nodules," *American journal of roentgenology*, vol. 174, pp. 71–74, 2000, [Online]. Available: www.macnet.or.jp/jsrt2/
2. P. Campadelli, E. Casiraghi, and D. Artioli, "A fully automated method for lung nodule detection from postero-anterior chest radiographs," *IEEE Trans Med Imaging*, vol. 25, no. 12, pp. 1588–1603, Dec. 2006, doi: 10.1109/TMI.2006.884198.

3. M. Sezgin and B. ̈lent Sankur, "Survey over image thresholding techniques and quantitative performance evaluation," *J Electron Imaging*, vol. 13, no. 1, p. 220, Jan. 2004, doi: 10.1117/1.1631316.
4. E. Soleymanpour, H. R. Pourreza, E. Ansaripour, and M. S. Yazdi, "Fully Automatic Lung Segmentation and Rib Suppression Methods to Improve Nodule Detection in Chest Radiographs," *Journal of medical signals and sensor*, vol. 1, pp. 191–199, 2011.
5. W. S. H. M. Wan Ahmad, W. M. D. W Zaki, and M. F. Ahmad Fauzi, "Lung segmentation on standard and mobile chest radiographs using oriented Gaussian derivatives filter," *Biomed Eng Online*, vol. 14, no. 1, Mar. 2015, doi: 10.1186/s12938-015-0014-8.
6. W. Liu, J. Luo, Y. Yang, W. Wang, J. Deng, and L. Yu, "Automatic lung segmentation in chest X-ray images using improved U-Net," *Sci Rep*, vol. 12, no. 1, Dec. 2022, doi: 10.1038/s41598-022-12743-y.
7. P. Pattrapisetwong and W. Chiracharit, "Automatic Lung Segmentation in Chest Radiographs Using Shadow Filter and Local Thresholding," in *IEEE Conference on Computational Intelligence in Bioinformatics and Computational Biology (CIBCB)*, 2016, pp. 1–6.
8. W. L. Lee, K. Chang, and K. S. Hsieh, "Unsupervised segmentation of lung fields in chest radiographs using multiresolution fractal feature vector and deformable models," *Med Biol Eng Comput*, vol. 54, no. 9, pp. 1409–1422, Sep. 2016, doi: 10.1007/s11517-015-1412-6.
9. T. A. Ngo and G. Carneiro, "LUNG SEGMENTATION IN CHEST RADIOGRAPHS USING DISTANCE REGULARIZED LEVEL SET AND DEEP-STRUCTURED LEARNING AND INFERENCE," in *IEEE International Conference on Image Processing (ICIP)*, 2015, pp. 2140–2143.
10. S. Candemir *et al.*, "Lung segmentation in chest radiographs using anatomical atlases with nonrigid registration," *IEEE Trans Med Imaging*, vol. 33, no. 2, pp. 577–590, Feb. 2014, doi: 10.1109/TMI.2013.2290491.
11. Y. Shao, Y. Gao, Y. Guo, Y. Shi, X. Yang, and D. Shen, "Hierarchical lung field segmentation with joint shape and appearance sparse learning," *IEEE Trans Med Imaging*, vol. 33, no. 9, pp. 1761–1780, 2014, doi: 10.1109/TMI.2014.2305691.
12. R. Deshpande, R. E. Ramalingam, P. Chatzistergos, V. Jasani, and N. Chockalingam, "Semi-automated lung field segmentation in scoliosis radiographs: An exploratory study," *J Med Biol Eng*, vol. 35, no. 5, pp. 608–616, Oct. 2015, doi: 10.1007/s40846-015-0084-x.
13. O. I. Singh, O. James, T. Sinam, and T. R. Singh, "Local Contrast and Mean based Thresholding Technique in Image Binarization," *Int J Comput Appl*, vol. 51, no. 6, pp. 975–8887, 2012.
14. B. van Ginneken, M. B. Stegmann, and M. Loog, "Segmentation of anatomical structures in chest radiographs using supervised methods: A comparative study on a public database," *Med Image Anal*, vol. 10, no. 1, pp. 19–40, Feb. 2006, doi: 10.1016/j.media.2005.02.002.
15. T. R. Singh, S. Roy, O. I. Singh, T. Sinam, and K. M. Singh, "A New Local Adaptive Thresholding Technique in Binarization," *International Journal of Computer Science*, vol. 8, no. 6, 2011, [Online]. Available: www.IJCSI.org
16. S. S. Parveen and C. Kavitha, "A REVIEW ON COMPUTER AIDED DETECTION AND DIAGNOSIS OF LUNG CANCER NODULES," *International Journal of Computers & Technology*, vol. 3, no. 3, pp. 393–400, 2012, [Online]. Available: www.cirworld.com
17. L. Zheng and Y. Lei, "A Review of Image Segmentation Methods for Lung Nodule Detection Based on Computed Tomography Images," in *MATEC Web of Conferences*, EDP Sciences, Nov. 2018. doi: 10.1051/matecconf/201823202001.
18. S. Hu, E. A. Hoffman, and J. M. Reinhardt, "Automatic Lung Segmentation for Accurate Quantitation of Volumetric X-Ray CT Images," *IEEE Trans Med Imaging*, vol. 20, no. 6, 2001.
19. M. N. Saad, Z. Muda, N. S. Ashaari, and H. A. Hamid, "Image Segmentation for Lung Region in Chest X-ray Images using Edge Detection and Morphology," in *IEEE International Conference on Control System, Computing and Engineering*, 2014, pp. 46–51.
20. A. Dawoud, "Lung segmentation in chest radiographs by fusing shape information in iterative thresholding," *IET Computer Vision*, vol. 5, no. 3, pp. 185–190, May 2011, doi: 10.1049/iet-cvi.2009.0141.
21. Z. Shi, P. Zhou, L. He, T. Nakamura, Q. Yao, and H. Itoh, "Lung segmentation in chest radiographs by means of Gaussian kernel-based FCM with spatial constraints," in *6th International Conference on Fuzzy Systems and Knowledge Discovery, FSKD 2009*, 2009, pp. 428–432. doi: 10.1109/FSKD.2009.811.

22. T. Cootes, "An Introduction to Active Shape Models," in *Image Processing and Analysis*, Ed.R.Baldock and J.Graham, Eds., Oxford University Press, 2000, pp. 223–248.
23. S. A. Patil and V. R. Udupi, "Chest X-ray features extraction for lung cancer classification," *J Sci Ind Res (India)*, vol. 69, pp. 271–277, 2010.
24. A. M. R. Schilham, B. Van Ginneken, and M. Loog, "Multi-scale Nodule Detection in Chest Radiographs," in *International Conference on Medical Image Computing and Computer-Assisted Intervention*, 2003, pp. 602–609. [Online]. Available: http://www.isi.uu.nl
25. S. Juhász, Á. Horváth, L. Nikházy, and G. Horváth, "Segmentation of Anatomical Structures on Chest Radiographs," in *MEDICON 2010, IFMBE Proceedings 29*, 2010, pp. 359–362. [Online]. Available: www.springerlink.com
26. T. F. Cootes, A. Hill, C. J. Taylor, and J. Hastam, "Use of active shape models for locating structures in medical images," *Image Vis Comput*, vol. 12, no. 6, pp. 355–365, 1994.
27. P. Annangi, S. Thiruvenkadam, A. Raja, H. Xu, X. Sun, and L. Mao, "A REGION BASED ACTIVE CONTOUR METHOD FOR X-RAY LUNG SEGMENTATION USING PRIOR SHAPE AND LOW LEVEL FEATURES," in *IEEE International Symposium on Biomedical Imaging*, IEEE, 2010, pp. 892–895.
28. J.-S. Lee, H.-H. Wu, and M.-Z. Yuan, "Lung Segmentation for Chest Radiograph by Using Adaptive Active Shape Models," in *2009 Fifth International Conference on Information Assurance and Security*, IEEE Computer Society, 2009.
29. D. K. Lakovidis and M. Savelonas, "Active Shape Model Aided by Selective Thresholding for Lung Field Segmentation in Chest Radiographs," in *9th International Conference on Information Technology and Applications in Biomedicine*, [IEEE], 2009.
30. B. Van Ginneken, A. F. Frangi, J. J. Staal, B. M. Ter Haar Romeny, and M. A. Viergever, "Active shape model segmentation with optimal features," *IEEE Trans Med Imaging*, vol. 21, no. 8, pp. 924–933, Aug. 2002, doi: 10.1109/TMI.2002.803121.
31. S. Sun, C. Bauer, and R. Beichel, "Automated 3-D segmentation of lungs with lung cancer in CT data using a novel robust active shape model approach," *IEEE Trans Med Imaging*, vol. 31, no. 2, pp. 449–460, Feb. 2012, doi: 10.1109/TMI.2011.2171357.
32. D. Kanade and J. Helonde, "Suppressing Chest Radiograph Ribs for Improving Lung Nodule Visibility by using Circular Window Adaptive Median Outlier (CWAMO)." [Online]. Available: www.ijacsa.thesai.org